Aalborg Universitet

AALBORG UNIVERSITY
DENMARK

Optimum Design of Power Converter Current Controllers in Large-Scale Power Electronics Based Power Systems

Ebrahimzadeh, Esmaeil; Blaabjerg, Frede; Wang, Xiongfei; Bak, Claus Leth

Optimum Design of Power Converter Current Controllers in Large-Scale Power Electronics Based Power Systems

Esmaeil Ebrahimzadeh
Member, IEEE
Department of Energy
Technology
Aalborg University
ebb@et.aau.dk

Frede Blaabjerg
Fellow, IEEE
Department of Energy
Technology
Aalborg University
fbl@et.aau.dk

Xiongfei Wang
Senior Member, IEEE
Department of Energy
Technology
Aalborg University
xwa@et.aau.dk

Claus Leth Bak
Senior Member, IEEE
Department of Energy
Technology
Aalborg University
clb@et.aau.dk

Abstract—**In a large-scale power electronic system like a wind farm, the mutual interactions between the power converter controllers and passive components may lead to instability problems or undesired dynamic response. This paper presents an optimum parameter design procedure for the power converter controllers in a power electronic system in order to guarantee a stable operation and to guarantee an acceptable dynamic response. In the approach, first, all oscillatory modes are calculated by a Multi-Input Multi-Output (MIMO) transfer function matrix of the power system; then, a multi-objective optimization procedure based on the Genetic Algorithm (GA) is presented to place the modes in the desired locations in order to increase the stability margin and to improve the dynamic response. Time-domain simulations of a 400-MW wind farm in the PSCAD/EMTDC environment confirms the effectiveness of the presented design approach.**

Keywords— *power electronic system, grid-connected converters, stability, dynamic response, design, optimization, damping*

I. INTRODUCTION

The fast growth of renewable energy sources, HVDC systems, variable-speed drivers, etc., has brought concerns about the stable and reliable operation of the future power system [1]-[6]. A power electronic system containing many power converters may show an undesired dynamic behavior or even an unstable operation, while the individual power converters show an acceptable dynamic characteristic for a strong grid. Recently, Transmission System Operators (TSOs) in different countries have reported a few times that they could not connect a wind farm to the grid because of harmonic-frequency oscillations [7]. In such cases, individual wind turbines have already passed different tests but the whole wind farm does not show a stable operation. The dynamic oscillations above the fundamental frequency are mainly coming from the mutual interactions between the high-bandwidth controllers and the passive components of the system [8], [9]. Therefore, this paper presents a method for designing the power converters to reduce the electrical oscillations by considering some information of the power system. There are two general approaches to analyze a power electronic system: One is the non-linear time-domain simulation analysis, which is accurate in a wide frequency range but has high computational burden. The second approach is the linearized frequency-domain analysis, which is accurate in the intended frequency range and

has low computational burden [10], [11]. Optimization of a large-scale power electronic system in the time-domain is complex because of too high computational burden. So far, frequency-domain analysis based on the state-space modeling has been done in various power electronic systems like microgrids, current source converters, and parallel voltage source inverters [12]- [16]. However, the state-space modeling can be complex for large-scale power electronic systems because it needs the information of each component of the system in details [17]- [21]. Another tool, for dynamic analysis of the system in the frequency-domain, is the impedance based modeling [22]-[27]. In this method, the source output impedance (Z_s) and the load input impedance (Z_l) are obtained and then the interconnected system stability is assessed by the Nyquist criterion of the ratio of $Z_l(s)/Z_s(s)$ [22]- [27]. Therefore, it can just identify if the system is stable and can not identify how much the stability margin is. So, the impedance-based analysis can not be used as a powerful design tool for a large number of power converters in a large-scale power electronic system.

In order to reduce the electrical oscillations and to improve the dynamic response in a large power electronic system, this paper presents a frequency-domain based optimum design method, which is simple and has low computational burden. The proposed optimized design approach is solved by using Genetic Algorithm (GA) and its objective function is to increase the stability margin and to improve the dynamic response. A large-scale power electronics based system is introduced as a Multi-Input Multi-Output (MIMO) transfer function matrix, which is simpler than state-space modeling. The dynamic analysis, the damping and frequencies of oscillatory modes are identified based on the determinant of the MIMO matrix.

In Section II, a grid-connected power electronic converter is modeled by a Norton equivalent circuit, i.e., a current source with a parallel active admittance. In Section III, a large power electronic system is modeled by a MIMO transfer function matrix. The proposed optimized parameter design is explained in Section IV, where the oscillatory modes of the system are placed in desired locations. In Section IV, a 400-MW wind farm is considered as a case study. In Section V, the proposed optimum design is tested by time-domain simulations of the 400-MW wind farm studied using the PSCAD/EMTDC

This article has been accepted for publication in a future issue of this journal, but has not been fully edited. Content may change prior to final publication. Citation information: DOI 10.1109/TIA.2018.2886190, IEEE Transactions on Industry Applications

2

environment software.

II. ADMITTANCE MODEL OF GRID-CONNECTED CONVERTER

A simple block-diagram of a grid-connected converter with an inner control loop is shown in Fig. 1(a), where $G_{cont\text{-}k}$ is the current controller, and $G_{delay\text{-}k}$ is the delay of the digital control implementation. Fig. 1(b) shows the block-diagram of the current closed-loop control system, where the PoC voltage ($V_{PoC\text{-}k}$) and the current reference ($I_{ref\text{-}k}$) are the inputs and the grid current ($I_{g\text{-}k}$) is the output. From Fig. 1(b), the grid current can be obtained from

$$I_{g-k} = G_{c-k}I_{ref-k} - Y_{c-k}V_{PoC-k} \tag{1}$$

where $G_{c\text{-}k}$ and $Y_{c\text{-}k}$ are

$$G_{c-k} = \frac{T_{c-k}}{1+T_{c-k}}, Y_{c-k} = \frac{Y_{Lf-k}}{1+T_{c-k}} \tag{2}$$

$T_{c\text{-}k}$ and $Y_{Lf\text{-}k}$ are

$$T_{c-k} = G_{cont-k}G_{delay-k}Y_{Lf-k}, Y_{Lf-k} = \frac{1}{sL_{f-k}} \tag{3}$$

Based on Equation (1), a grid-connected converter can be modeled by an ideal current source along with a parallel active admittance (Norton equivalent circuit) as shown in Fig. 1(c). This paper focuses on optimum design of the current controller, which is fast and a high-bandwidth controller. Therefore, the outer power controllers and grid synchronization loops are neglected as they are too slow to have influence on current controller dynamics. In this paper, $G_{cont\text{-}k}$ is considered to be a Proportional plus Resonant (PR) current controller and $G_{delay\text{-}k}$ is modeled by Pade approximation, i.e.,

$$G_{cont-k} = K_{p-k} + \frac{K_{i-k}s}{s^2 + \omega_f^2}$$

$$G_{delay-k}(s) = e^{-1.5T_{s-k}s} \approx \frac{1 - \frac{1.5T_{s-k}}{2}s + \frac{(1.5T_{s-k})^2}{12}s^2}{1 + \frac{1.5T_{s-k}}{2}s + \frac{(1.5T_{s-k})^2}{12}s^2} \tag{4}$$

where ω_f is the fundamental frequency and $T_{s\text{-}k}$ is the sampling period of the digital control.

(a) grid-connected converter with the inner control loop

(b) closed-loop control of grid current

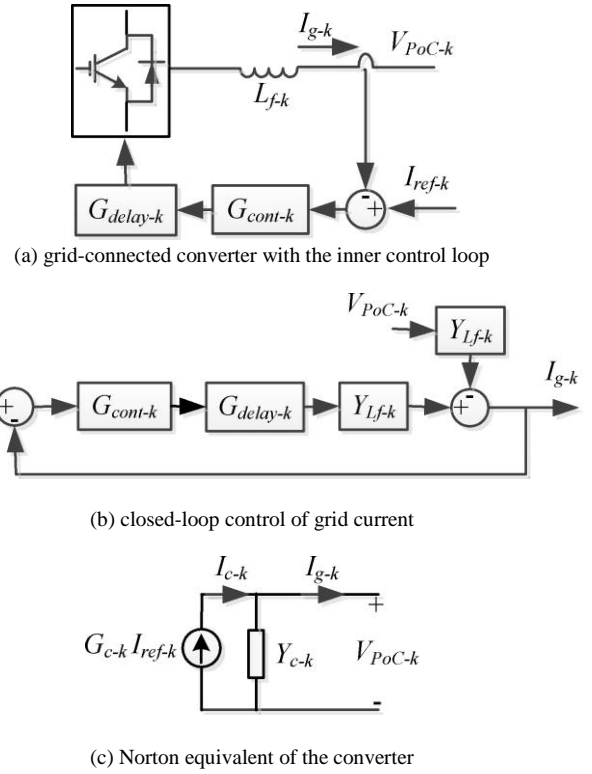(c) Norton equivalent of the converter

Fig. 1. Grid-connected converter with the inner control loop and its equivalent circuit.

III. A POWER ELECTRONIC SYSTEM AS A MULTI-INPUT MULTI-OUTPUT (MIMO) TRANSFER FUNCTION MATRIX

By modeling of every passive element and active element (power electronic converters) as Norton equivalent circuit, the current-voltage relationships in a power electronic system can be obtained by the nodal admittance matrix as given in (5). In (5), it is assumed that bus *1* is connected to the electrical grid and bus *2* to bus *n+1* are connected to the power electronic converters. $Y_{c\text{-}k}$ (k=1,2, ...,n), $Y_{ii}, Y_{ij}(s)$ (i,j=1,2, ...,m, and i≠j) are the active admittance of the kth power electronic converter, the connected admittance to the ith bus, the admittance between i^{th} bus and j^{th} bus, respectively. When a component model is black-box, its equivalent admittance can be obtained by

$$\begin{bmatrix} I_g \\ I_{c-1} \\ I_{c-2} \\ \vdots \\ I_{c-n} \\ 0 \\ \vdots \\ 0 \end{bmatrix} = \begin{bmatrix} Y_{11} & -Y_{12} & -Y_{13} & \cdots & -Y_{1(n+1)} & -Y_{1(n+2)} & \cdots & -Y_{1m} \\ -Y_{21} & Y_{22}+Y_{c-1} & -Y_{23} & \cdots & -Y_{2(n+1)} & -Y_{2(n+2)} & \cdots & -Y_{2m} \\ -Y_{31} & -Y_{32} & Y_{33}+Y_{c-2} & \cdots & -Y_{3(n+1)} & -Y_{3(n+2)} & \cdots & -Y_{3m} \\ \vdots & \vdots & \vdots & \vdots & \vdots & \vdots & \vdots & \vdots \\ -Y_{(n+1)1} & -Y_{(n+1)2} & -Y_{(n+1)3} & \cdots & Y_{(n+1)(n+1)}+Y_{c-n} & Y_{(n+1)(n+2)} & \cdots & -Y_{(n+1)m} \\ -Y_{(n+2)1} & -Y_{(n+2)2} & -Y_{(n+2)3} & \cdots & -Y_{(n+2)(n+1)} & Y_{(n+2)(n+2)} & \cdots & -Y_{(n+2)m} \\ \vdots & \vdots & \vdots & \vdots & \vdots & \vdots & \vdots & \vdots \\ -Y_{m1} & -Y_{m2} & -Y_{m3} & \cdots & -Y_{mn} & -Y_{m(n+2)} & \cdots & Y_{mm} \end{bmatrix} \begin{bmatrix} V_1 \\ V_2 \\ V_3 \\ \vdots \\ V_n \\ V_{(n+1)} \\ \vdots \\ V_m \end{bmatrix} \tag{5}$$

experiment (if the component has been built) or by numerical simulations (if the component has been designed but has not been built yet). Equation (5) is actually a Multi-Input Multi-Output (MIMO) transfer function matrix [28], where the outputs are the bus voltages and the inputs are the injected currents, i.e,

$$\mathbf{V(s) = G(s)^{-1} I(s)} \qquad (6)$$

The poles of the introduced MIMO transfer function can be calculated by solving the following equation:

$$\det\left[\mathbf{G(s)}\right] = 0$$
$$\Rightarrow p_1 = \alpha_1 + j\beta_1, p_2 = \alpha_2 + j\beta_2, \cdots, p_q = \alpha_q + j\beta_q \qquad (7)$$

where the frequency (f_i) and the damping ratio (ζ_i) of the poles can be obtained from

$$f_i = \frac{\beta_i}{2\pi} \qquad \zeta_i = \frac{-\alpha_i}{\sqrt{\alpha_i^2 + \beta_i^2}} \qquad (8)$$

The poles of the MIMO transfer function matrix basically are the poles of its elements, i.e,

$$G_{ij}(s) = \frac{P(s)}{(s-p_1)(s-p_2)\cdots(s-p_q)}$$
$$= \frac{A_1}{(s-p_1)} + \frac{A_2}{(s-p_2)} + \cdots + \frac{A_q}{(s-p_q)} \qquad (9)$$
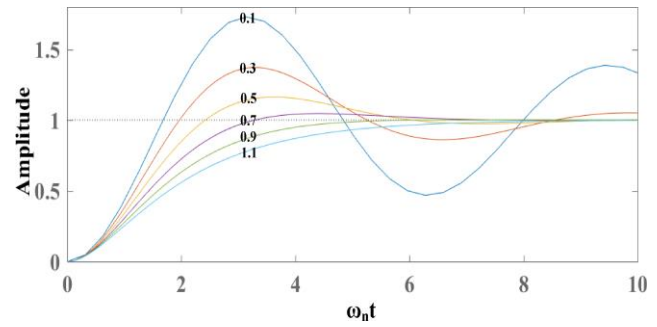

Fig. 2. Step response of a simple second-order system for different damping ratios.

The inverse Laplace transform of $G_{ij}(s)$ is

$$G_{ij}(t) = A_1 e^{p_1 t} + A_2 e^{p_2 t} + \cdots + A_q e^{p_q t}$$
$$= A_1 e^{\alpha_1 t} e^{j\beta_1 t} + A_2 e^{\alpha_2 t} e^{j\beta_2 t} + \cdots + A_q e^{\alpha_q t} e^{j\beta_q t} \qquad (10)$$

Therefore, the poles of $G_{ij}(s)$ in the s-domain are related to the oscillations of the system in the time-domain. The imaginary parts of the poles identify the frequencies of oscillations and the real parts identify the damping of the oscillations. If α_q (one of the real parts) is positive, the term $A_q e^{\alpha_q t} e^{j\beta_q t}$ is a function with an increasing exponential magnitude and the system is unstable. If α_q is negative, the term $A_q e^{\alpha_q t} e^{j\beta_q t}$ is a decaying exponential function with a final value of zero.
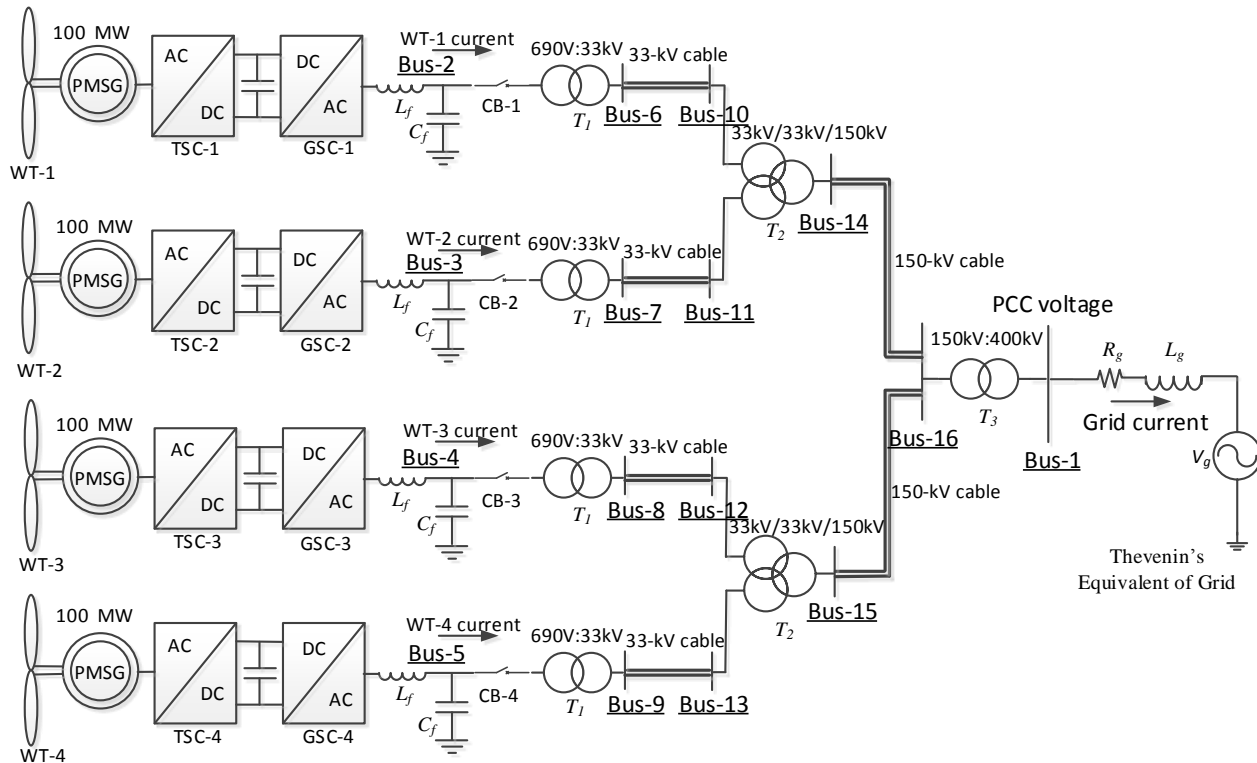

Fig. 3. 400-MW wind farm, which is studied for the proposed optimum controller design method.

IV. PROPOSED OPTIMUM DESIGN OF CURRENT CONTROLLER

A. Guaranteeing stability

According to the previous discussion, a power electronics based system is stable if and only if all its poles (P_1, P_2, ..., and P_q) have negative real parts. The mode with the largest real part can be found by

$$P_c = \alpha_c + j\beta_c \quad \alpha_c = Max(\alpha_1, \alpha_2, \cdots, \alpha_q) \tag{11}$$

If P_c has a negative real part, it means that the real parts of all modes are negative. Therefore, in order to guarantee the stability, an inequality constraint, H(x), is considered in GA algorithm to set the real part of P_c smaller than zero. The threshold value for stability is zero mathematically. However, because of the round-off errors of floating-point computations and the grid variations, the threshold value should be considered a value larger than zero to be robust. So, it is considered to be ten here., i.e.,

$$\alpha_c + 10 = H(\mathbf{x}) \leq 0 \tag{12}$$

where **x**, optimization variable, can be a vector including the current controller and filter parameters of the grid-connected converter.

$$\mathbf{x} = [K_p, K_i, L_f, C_f] \tag{13}$$

The optimum parameter vector (**x**) includes the filter parameters to have more freedom degrees and to optimize the system ideally. In a case, if the filter parameters can not be redesigned, the vector includes only the controller parameters. In this case, there are less freedom degrees for the optimization and may not optimize the system ideally.

B. Guaranteeing the desired dynamic performance

Fig. 2 shows the step response of a simple second-order system for different damping ratios, which is used as an example for evaluating the dynamic response of a system. Fig. 2 shows that the amount of overshoot depends on the damping ratio. The system with a smaller damping ratio reaches the final value faster, but the response oscillates around this final value. A system with a damping ratio around 0.8 can be a good trade-off between the speed and oscillation of the response as shown in Fig. 2.

In a power electronics based systems, low-frequency modes are related to the power converter controllers and the high-frequency modes are more related to the cables and transformers. As the switching frequency (f_s) is considered to be 2.5 kHz, the maximum logical bandwidth for the current controller would be around 500 Hz ($f_s/5$) [29]. Therefore, In order to guarantee the desired dynamic performance of the power converters in a power electronic system, an objective function is considered to set the damping ratios of all low-frequency modes close to 0.8; in fact, the objective function is to minimize F(x) as described in (14).

$$F(x) = Max\left[|\zeta_1 - 0.8|, |\zeta_2 - 0.8|, \cdots, |\zeta_n - 0.8|\right]$$

$$\zeta_j = \frac{-\alpha_j}{\sqrt{\alpha_j^2 + \beta_j^2}}, f_j = \frac{\beta_j}{2\pi} < f_{h1} \cong 500Hz, j = 1,2,...,n \tag{14}$$
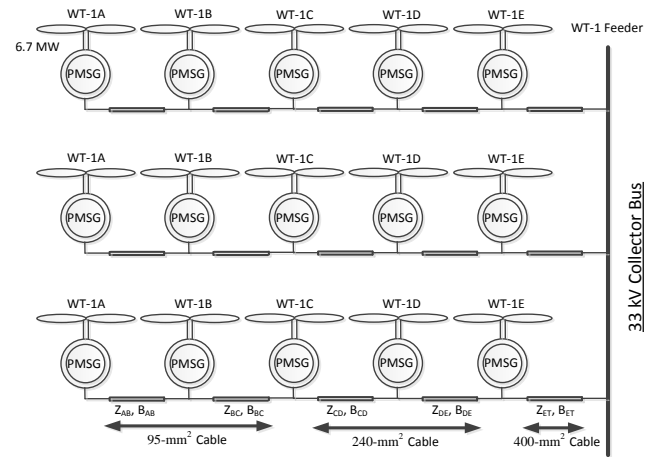

Fig. 4. Fifteen wind turbines, which are located on each 100-MW string of the wind farm shown in Fig. 3.
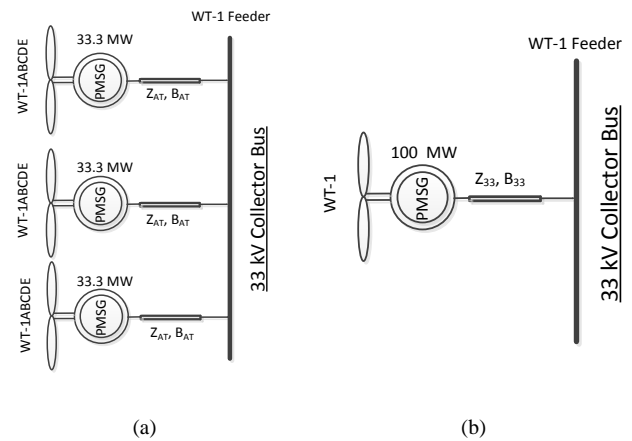

(a)   (b)

Fig. 5. Aggregated model of the fifteen wind turbines shown in Fig. 4, (a) aggregated model on each feeder, (b) aggregated model of three feeders.

V. A 400-MW WIND FARM AS A CASE STUDY

The effectiveness of the proposed optimized design approach is studied for a 400-MW wind farm with 100-MW aggregated strings, as shown in Fig. 3. Fifteen Wind Turbines (WTs) of 6.7 MW are located on three parallel feeders as shown in Fig. 4.

Under the nominal operation, the current on the feeder is increasing towards the collector bus as the number of the WTs is also increasing. Therefore, a closer cable to the collector bus should have larger cross-section than a farther cable. Consequently, three different cables (95 mm² cable, 240 mm² cable, and 400 mm² cable) carry the feeder current. Five WTs of 6.7-MW on each feeder can be aggregated by one 33-MW WT as shown in Fig. 5(a). If it is assumed that the injected power by the WTs on the feeder are the same, the equivalent impedance parameters of the 33-MW WT can be calculated by

$$Z_{AT} = \frac{Z_{AB} + 4Z_{BC} + 9Z_{CD} + 16Z_{DE} + 25Z_{ET}}{25}$$

$$B_{AT} = B_{AB} + B_{BC} + B_{CD} + B_{DE} + B_{ET} \tag{15}$$

where, Z_{AT} and B_{AT} are the equivalent series impedance and the equivalent shunt susceptance, respectively. Z_{AB}, Z_{BC}, Z_{CD},
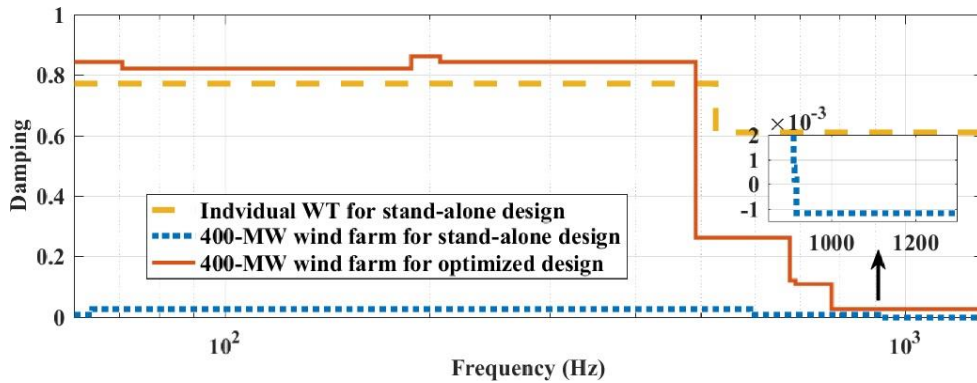
Fig. 7. Mode damping ratios of the individual WT and the wind farm for the stand-alone design, and for the optimum design.
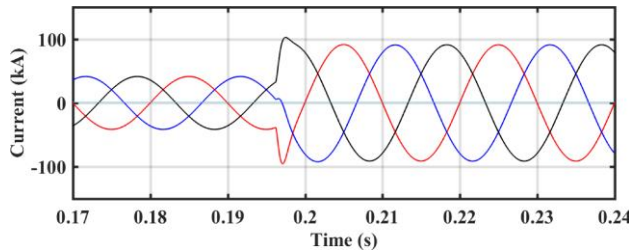

Fig. 6. Step-response of the designed GSC for a strong grid.

Table I. Parameters of the 400-MW wind farm and Genetic Algorithm (GA) Solver

Parameter		Value
Transformer T₁	Leakage inductance	1.378 µH
Cable ₃₃-kv	Shunt capacitance	3.24 µF
	Series inductance	0.436 mH
	Series resistance	0.0537 Ω
Transformer T₂	Leakage inductance	1.891 mH
Cable ₁₅₀-kv (Cable length = 10 km)	Shunt capacitance	0.26 µF/km
	Series inductance	0.5 mH/km
	Series resistance	0.0574 Ω/km
Transformer T₃	Leakage inductance	22.788 mH
Grid	X/R ratio	20
	SCR	100
Current controller	Kₚ	2.5e-3
	Kᵢ	2
	fₛ	2.5 kHz
Genetic Algorithm (GA) Solver	Population Size	40
	Generations	160
	Stall Generations	80
	Function Tolerance	1 ×10⁻⁵

Z_{DE}, and Z_{ET} are the series impedances of the sections and B_{AB}, B_{BC}, B_{CD}, B_{DE}, and B_{ET} are the shunt susceptances (see Fig. 4). Finally, the aggregated 33.3-MW WTs on three parallel feeders can be aggregated as one 100-MW WT (see Fig. 5(b)). The equivalent series impedance and shunt susceptance can be calculated by

$$Z_{33} = \frac{Z_{AT}}{3} \qquad B_{33} = 3B_{AT} \qquad (16)$$

Since the dc-link is almost constant, the dynamics of the Turbine-Side Converters (TSCs) can be neglected. A simple Thévenin equivalent voltage source is used to represent the grid. The transformers are modeled by its short-circuit impedances and the cables are modeled by the nominal π-

Fundamental (50Hz) = 566.1 , THD= 12.05%

(a)

(b)
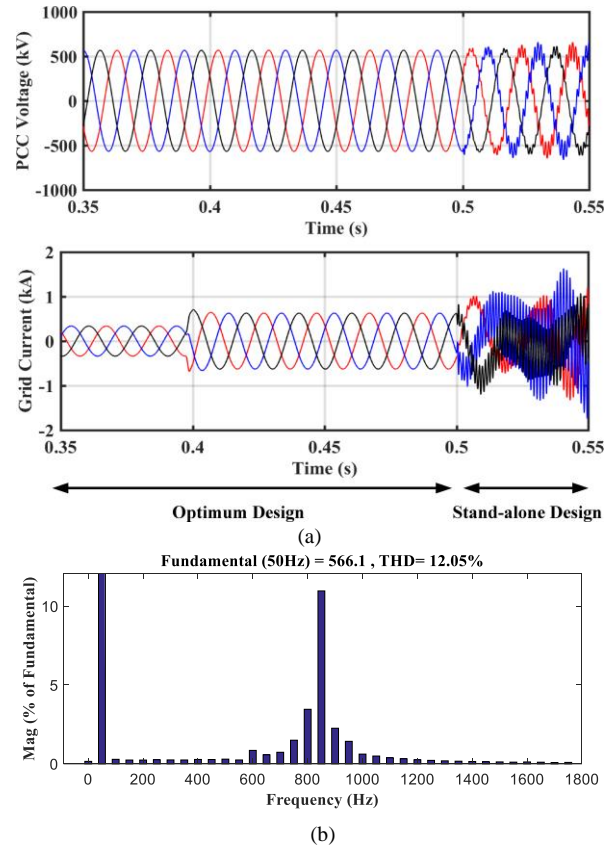
Fig. 8. Dynamic response of GSC. GSC parameters are changed from the optimum design to the initial design at t = 0.5 s and the dynamic response of the optimum design is also tested at t = 0.4 s, (a) PCC voltage and gird current, (b) FFT analysis of PCC voltage between t = 0.52s to t = 0.54s.

model. The parameters of the wind farm are given in Table I. Short Circuit Ratio (SCR) is defined by

$$SCR = \frac{V_g^2}{Z_g S_{base}} \qquad (17)$$

Where V_g and Z_g are the grid voltage and the grid impedance, and S_{base} is the apparent power injected by the wind farm. For large X/R ratio, $Z_g = X_g = \omega_0 L_g$. More detailed information about the model can be found in [29]. The current controller and filter parameters of the Grid-Side Converters (GSCs) are
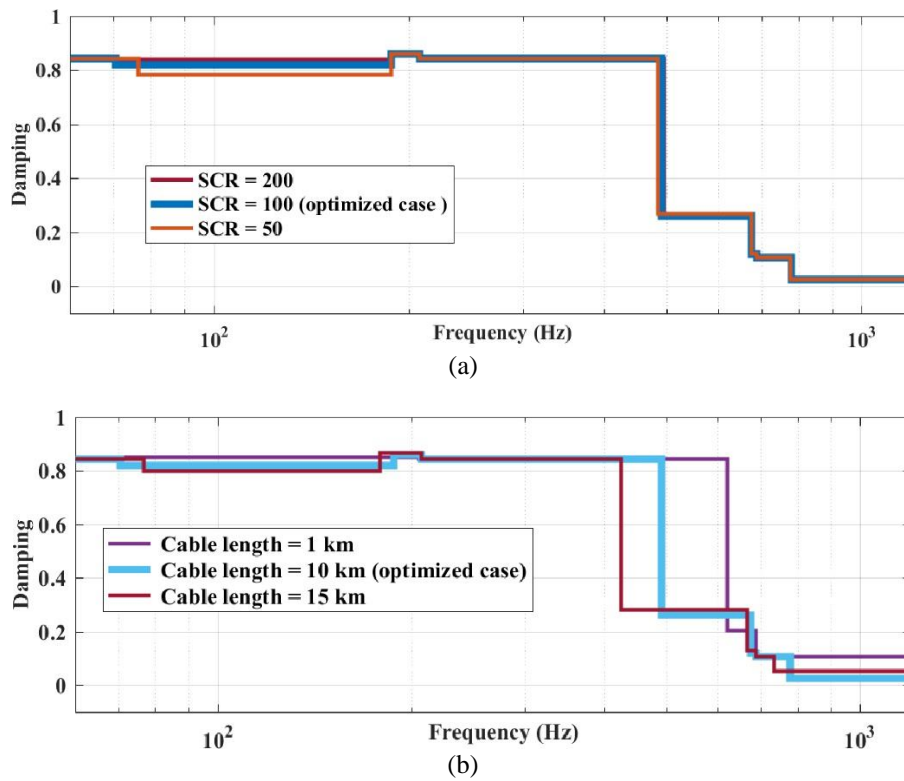
Fig. 9. Robustness of the optimum design case (SCR = 100 and Cable length = 10 km) against variations, (a) SCR = 100 (optimized case) is changed to SCR =50 and SCR =200, (b) Cable length = 10 km (optimized case) is changed to Cable length = 1 km and Cable length = 15 km.

designed for a desired phase-margin of 45° for stand-alone operation. Fig. 6 shows the step-response of the GSC for a strong grid, where a desired dynamic response can be observed. The same controllers are used for all GSCs.

VI. Proposed Optimum Design in Frequency-domain and Corresponding Time-domain Simulations

A. Optimum design

Fig. 7 shows the mode damping ratios of the individual WT and the wind farm for the stand-alone design (initial design). The damping ratios of the modes of the wind farm for the optimized parameters ($K_p = 9.51e$-3, $K_i = 4.16$, and $f_{res} = 357$ Hz) are also shown in Fig. 7. As it can be seen, the damping ratios of the individual WT for the stand-alone design is around 0.8, which confirms that the individual WT for a strong grid has a good stability margin and an acceptable dynamic response. However, when all WTs are connected to the wind farm, the damping ratios for low-frequency modes are too small and the damping ratio for frequency around 900 Hz is negative, which shows that the wind farm is unstable around this frequency. Therefore, it is necessary to redesign the controller parameters to improve the stability margin and to guarantee a desired dynamic response. As shown in Fig. 7, after setting the GSC parameters based on the proposed optimum design procedure, all modes have positive damping, which confirms that the wind farm has a stable operation. In addition, the low-frequency modes, which is related to the power converter dynamics, have suitable dampings around 0.8, which depicts that the wind farm has a desired dynamic performance for the optimum design.
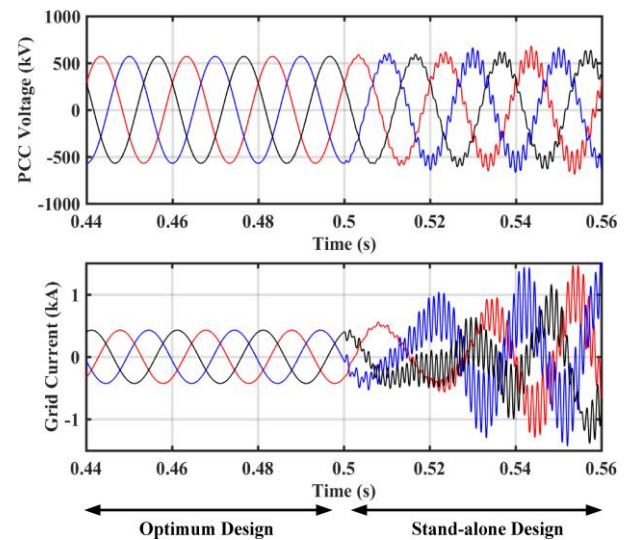
Fig. 10. Robustness of the optimum design. The GSC parameters are optimized and set for SCR = 100 and Cable length = 10 km but the wind farm is simulated for another case, i.e., SCR = 50 and Cable length = 15 km. At t = 0.5, the GSC parameters are changed to the initial design

In Fig. 8, the wind farm is simulated in the time-domain using PSCAD software, where the current controller parameters of the GSCs have been set by the proposed optimum design (before t = 0.5 s). At t = 0.4 s, the current reference is changed from 0.25 p.u. to 1 p.u. As it can be seen, the wind farm has a good dynamic response and a stable operation for the optimized parameters. At t = 0.5, the GSC parameters are changed from the optimum design to the initial design. As shown in Fig. 8,

some oscillations around 900 Hz propagate into the wind farm, because of the instability problems as predicted in Fig. 7 in the frequency-domain. Therefore, it can be concluded that a good control design for an individual power converter cannot guarantee the stable operation of the whole power electronics based system as shown in Fig. 8.

B. Sensitivity analysis with respect to system variations

In this section, the robustness of the optimum design case (SCR = 100 and Cable length = 10 km) against variations of the wind farm is studied. Fig. 9(a) shows the mode damping ratios of the wind farm, where SCR = 100 (optimized case) is changed to SCR =50 and SCR =200. Fig. 9(b) shows the mode damping ratios, where Cable length = 10 km (optimized case) is changed to Cable length = 1 km and Cable length = 15 km. As it can be seen, the damping ratios of modes, particularly low-frequency modes, are not affected a lot against such variations. The high frequency poles are related to the resonance modes resulting from the capacitance and the inductance of the cables. By increasing the cable length, the capacitance and the inductance of the cable increase and the resonance frequency decreases. The damping of these poles is corresponded to the resistance of the cable. As this resistance is very small, the damping of these poles is small. In order to confirm the robustness of the optimized design, the time-domain simulations have also been performed. First, the GSC parameters are optimized and set for SCR = 100 and Cable length = 10 km. However, the wind farm is simulated for another SCR and cable lengths, i.e., SCR = 50 and Cable length = 15 km. At t = 0.5, the parameters are changed to the initial design. As it can be seen from Fig. 10, the wind farm with the optimum controller design presents a robust and stable operation. However, after t = 0.5, the wind farm with the initial parameters is unstable and harmonic-frequency oscillations propagate into the grid.

VII. Conclusion

This paper presents a multi-objective design procedure for the power converter controllers in order to increase the stability margin in a power electronics based system. A power electronic system is introduced as a Multi-Input Multi-Output (MIMO) transfer function matrix and the oscillatory modes are identified by the determinant of the MIMO matrix. The proposed algorithm put the modes in the desired locations to improve the dynamic response of the system. A 400-MW wind farm is studied as a power electronics based system for the proposed optimum design procedure. Time-domain simulations confirm that a good design for an individual converter under strong grid cannot guarantee a stable operation of the whole power electronic system including many other converters and passive components. On the other hand, the proposed design technique is a powerful tool to analyze and to improve the dynamic performance of a large-scale power electronic system like a wind farm. In addition, the power electronic system with the optimum controller design shows a robust and stable operation against variations of the system.

References

[1] B. K. Bose, "Global energy scenario and impact of power electronics in 21st century," *IEEE Trans. Ind. Electron.*, vol. 60, no. 7, pp. 2638–2651, Jul. 2013.

[2] F. Blaabjerg, R. Teodorescu, M. Liserre, and A. V. Timbus, "Overview of control and grid synchronization for distributed power generation systems," *IEEE Trans. Ind. Electron.*, vol. 53, no. 5, pp. 1398–1409, Oct. 2006.

[3] J. Liu, T. A. Nondahl, P. B. Schmidt, S. Royak, and T. M. Rowan, "Generalized stability control for open-loop operation of motor drives," *IEEE Trans. Ind. Appl.*, vol. 53, no. 3, pp. 2517-2525, Jun. 2017.

[4] L. Wang, Z. H. Yang, X. Y. Lu, and A. V. Prokhorov, "Stability analysis of a hybrid multi-infeed HVdc system connected between two offshore wind farms and two power grids," *IEEE Trans. Ind. Appl.*, vol. 53, no. 3, pp. 1824-1833, Jun. 2017.

[5] Y. Guan, J. C. Vasquez, J. M. Guerrero, Y. Wang, and W. Feng, "Frequency stability of hierarchically controlled hybrid photovoltaic-battery-hydropower microgrids," *IEEE Trans. Ind. Appl.*, vol. 51, no. 6, pp. 4729-4742, Dec. 2015.

[6] K. N. B. M. Hasan, K. Rauma, A. Luna, J. I. Candela, and P. Rodriguez,"Harmonic compensation analysis in offshore wind power plants using hybrid filters," *IEEE Trans. Ind. Appl.*, vol. 50, no. 3, pp. 2050–2060, Jun. 2014.

[7] C. F. Jensen, Ł. H. Kocewiak, Z. Emin, "Amplification of harmonic background distortion in wind power plants with long high voltage connections," *CIGRE Biennial Session, CIGRÉ*, 21-26 August 2016, Paris, France, C4-112.

[8] C. Yoon, H. Bai, R. Beres, X. Wang, C. Bak, and F. Blaabjerg, "Harmonic stability assessment for multi-paralleled, grid-connected inverters," *IEEE Trans. Sustain. Energy,* vol. 7, no. 4, pp. 1388-1397, Oct. 2016.

[9] A. Rygg, M. Molinas, C. Zhang, and X. Cai, "A modified sequence-domain impedance definition and its equivalence to the dq-domain impedance definition for the stability analysis of AC power electronic systems," *IEEE Trans. Emerg. Sel. Topics Power Electron.,* vol. 4, no. 4, pp. 1383-1396, Dec. 2016.

[10] B. Badrzadeh, M. Gupta, N. Singh, A. Petersson, L. Max, and M. Høgdahl, "Power system harmonic analysis in wind power plants — Part I: Study methodology and techniques," in *Proc. of IEEE IAS*, 2012, pp. 1-11.

[11] N. Bottrell, M. Prodanovic, and T. C. Green, "Dynamic stability of a microgrid with an active load," *IEEE Trans. Power Electron.,* vol. 28, no.11, pp. 5107-5119, Nov. 2013.

[12] A. Singh, and A. K. Kaviani, and B. Mirafzal, "On dynamic models and stability analysis of three-phase phasor PWM-based CSI for stand-alone applications," *IEEE Trans. Ind. Electron.,* vol. 62, no. 5, pp. 2698-2707, May. 2015.

[13] L. P. Kunjumuhammed, B. C. Pal, C. Oates, and K. J. Dyke, "Electrical oscillations in wind farm systems: analysis and insight based on detailed modeling," *IEEE Trans. Sustain. Energy,* vol. 7, no. 1, pp. 51–62, Jan. 2016.

[14] J. B. Kwon, X. Wang, F. Blaabjerg, C. L. Bak, A. R. Wood and N. R. Watson, "Harmonic instability analysis of a single-phase grid-connected converter using a harmonic state-space modeling method," *IEEE Trans. Ind. Appl.,* vol. 52, no. 5, pp. 4188-4200, Sept.-Oct. 2016.

[15] A. Guha and G. Narayanan, "Small-signal stability analysis of an open-loop induction motor drive including the effect of inverter deadtime," *IEEE Trans. Ind. Appl.,* vol. 52, no. 1, pp. 242-253, Feb. 2016.

[16] E. A. A. Coelho, P. C. Cortizo, and P. F. D. Garcia, "Small-signal stability for parallel-connected inverters in stand-alone AC supply systems," *IEEE Trans. Ind. App.,* vol. 38, no. 2, pp. 533-542, Mar. 2002.

[17] L. P. Kunjumuhammed, B. C. Pal, C. Oates, and K. J. Dyke, "The adequacy of the present practice in dynamic aggregated modeling of wind farm systems," *IEEE Trans. Sustain. Energy*, vol. 8, no. 1, pp. 23-32, Jan. 2017.

[18] E. Ebrahimzadeh, F. Blaabjerg, X. Wang, and C. L. Bak, "Harmonic stability and resonance analysis in large PMSG-based wind power plants," *IEEE Trans. Sustain. Energy*, vol. 9, no. 1, pp. 12-23, Jan. 2018.

[19] E. Ebrahimzadeh, F. Blaabjerg, X. Wang and C. L. Bak, "Bus participation factor analysis for harmonic instability in power electronics based power systems," *IEEE Trans. Power Electron.*, vol. 33, no. 12, pp. 10341-10351, Dec. 2018.

This article has been accepted for publication in a future issue of this journal, but has not been fully edited. Content may change prior to final publication. Citation information: DOI 10.1109/TIA.2018.2886190, IEEE Transactions on Industry Applications

8

[20] L. P. Kunjumuhammed, B. C. Pal, C. Oates, and K. J. Dyke, "Electrical oscillations in wind farm systems: analysis and insight based on detailed modeling," *IEEE Trans. Sustain. Energy*, vol. 7, no. 1, pp. 51–62, Jan. 2016.

[21] E. Ebrahimzadeh, F. Blaabjerg, X. Wang, and C. L. Bak, "Modeling and identification of harmonic instability problems in wind farms," *in Proc. 2016 IEEE Energy Conversion Congress and Expo. (ECCE),* Milwaukee, WI, pp. 1

[22] J. Sun, "Impedance-based stability criterion for grid-connected inverters," *IEEE Trans. Power Electron.*, vol. 26, no. 11, pp. 3075–3078, Nov. 2011.

[23] L. Harnefors, R. Finger, X. Wang, H. Bai, and F. Blaabjerg, "VSC input-admittance modeling and analysis above the nyquist frequency for passivity-based stability assessment," *IEEE Trans. Ind. Electron.*, vol. 64, no. 8, pp. 6362-6370, Aug. 2017.

[24] X. Wang, F. Blaabjerg, and W. Wu, "Modelling and analysis of harmonic stability in ac power-electronics-based power system," *IEEE Trans. Power Electron.*, vol. 29, no. 12, pp.6421 -6432, Dec. 2014.

[25] M. Cespedes and J. Sun, "Impedance modeling and analysis of grid connected voltage-source converters," *IEEE Trans. Power Electron.,* vol. 29, no. 3, pp. 1254–1261, Mar. 2014.

[26] X. Wang, L. Harnefors, and F. Blaabjerg, "A unified impedance model of grid-connected voltage-source converters," *IEEE Trans. Power Electron.,* 2017, early access, doi: 10.1109/TPEL.2017.2684906

[27] L. Xu, L. Fan and Z. Miao, "DC impedance-model-based resonance analysis of a VSC–HVDC system," *IEEE Trans. Power Del.,* vol. 30, no. 3, pp. 1221-1230, Jun. 2015.

[28] S. Skogestad and I. Postlethwaite, "Multivariable feedback control: analysis and design, " New York: Wiley, 2000

[29] S. K. Chaudhary, "Control and protection of wind power plants with VSC-HVDC connection," PhD Thesis, Aalborg University, Aalborg, Denmark, 2011.

Esmaeil Ebrahimzadeh (S'16) received the M.Sc. degree in Electrical Engineering from University of Tehran, Tehran, Iran, where he has also been a lecturer for undergraduate courses. In 2015, he was employed as a PhD Fellow at the Department of Energy Technology, Aalborg University, Aalborg, Denmark, where he is currently an Industrial Postdoc. He has been a visiting R&D Engineer at Vestas Wind Systems A/S, Aarhus, Denmark, in 2017, where he is currently working as a R&D Control Engineer. His research interests include modeling, design, and control of power-electronic converters in different applications, as well as power quality and stability analysis in large wind power plants. He is an IEEE member and received the best paper awards at IEEE PEDG 2016 and IEEE PES GM 2017.

Frede Blaabjerg (S'86–M'88–SM'97–F'03) was with ABB-Scandia, Randers, Denmark, from 1987 to 1988. From 1988 to 1992, he got the PhD degree in Electrical Engineering at Aalborg University in 1995. He became an Assistant Professor in 1992, an Associate Professor in 1996, and a Full Professor of power electronics and drives in 1998. From 2017 he became a Villum Investigator. He is honoris causa at University Politehnica Timisoara (UPT), Romania and Tallinn Technical University (TTU) in Estonia.

His current research interests include power electronics and its applications such as in wind turbines, PV systems, reliability, harmonics and adjustable speed drives. He has published more than 600 journal papers in the fields of power electronics and its applications. He is the co-author of four monographs and editor of ten books in power electronics and its applications.

He has received 29 IEEE Prize Paper Awards, the IEEE PELS Distinguished Service Award in 2009, the EPE-PEMC Council Award in 2010, the IEEE William E. Newell Power Electronics Award 2014 and the Villum Kann Rasmussen Research Award 2014. He was the Editor-in-Chief of the IEEE TRANSACTIONS ON POWER ELECTRONICS from 2006 to 2012. He has been Distinguished Lecturer for the IEEE Power Electronics Society from 2005 to 2007 and for the IEEE Industry Applications Society from 2010 to 2011 as well as 2017 to 2018. In 2018 he is President Elect of IEEE Power Electronics Society. He serves as Vice-President of the Danish Academy of Technical Sciences.

He is nominated in 2014, 2015, 2016 and 2017 by Thomson Reuters to be between the most 250 cited researchers in Engineering in the world.

Xiongfei Wang (S'10-M'13-SM'17) received the B.S. degree from Yanshan University, Qinhuangdao, China, in 2006, the M.S. degree from Harbin Institute of Technology, Harbin, China, in 2008, both in electrical engineering, and the Ph.D. degree in energy technology from Aalborg University, Aalborg, Denmark, in 2013.

Since 2009, he has been with the Department of Energy Technology, Aalborg University, where he is currently a Professor and Research Program Leader for Electronic Grid Infrastructure. His research interests include modeling and control of grid-connected converters, harmonics analysis and control, passive and active filters, stability of power electronic based power systems.

Dr. Wang serves as an Associate Editor for the IEEE TRANSACTIONS ON POWER ELECTRONICS, the IEEE TRANSACTIONS ON INDUSTRY APPLICATIONS, and the IEEE JOURNAL OF EMERGING AND SELECTED TOPICS IN POWER ELECTRONICS. In 2016, he was selected into Aalborg University Strategic Talent Management Program for the next-generation research leaders. He received four IEEE prize paper awards, the outstanding reviewer award of IEEE TRANSACTIONS ON POWER ELECTRONICS in 2017, and the IEEE PELS Richard M. Bass Outstanding Young Power Electronics Engineer Award in 2018..

Claus Leth Bak was born in Århus, Denmark, on April 13th, 1965. He received the B.Sc. with honors in Electrical Power Engineering in 1992 and the M.Sc. in Electrical Power Engineering at the Department of Energy Technology at Aalborg University in 1994. After his studies he worked as a professional engineer with Electric Power Transmission and Substations with specializations within the area of Power System Protection at the NV Net Transmission System Operator. In 1999 he was employed as an Assistant Professor at the Department of Energy Technology, Aalborg University, where he holds a Full Professor position today. He received the PhD degree in 2015 with the thesis

"EHV/HV underground cables in the transmission system". He has supervised/co-supervised +35 PhD's and +50 MSc theses. His main Research areas include Corona Phenomena on Overhead Lines, Composite Transmission Towers, Power System Modeling and Transient Simulations, Underground Cable transmission, Power System Harmonics, Power System Protection and HVDC-VSC Offshore Transmission Networks. He is the author/coauthor of app. 310 publications. He is a member of Cigré SC C4 AG1 and SC B5 and chairman of the Danish Cigré National Committee (August 2018). He is an IEEE senior member (M'1999, SM'2007). He received the DPSP 2014 best paper award and the PEDG 2016 best paper award. He serves as Head of the Energy Technology PhD program (+ 120 PhD's) and as Head of the Section of Electric Power Systems and High Voltage and is a member of the PhD board at the Faculty of Engineering and Science.